Modeling of sodium nitrite and water transport in pork meat

J. Gómez[a], N. Sanjuán[b], J. Arnau[c], J. Bon[b], G. Clemente[b*]

[a]Departamento de Alimentos, División de Ciencias de la Vida, Campus Irapuato-Salamanca, Universidad de Guanajuato, Carretera Irapuato-Silao km 9, Ex-Hacienda El Copal, 36500 Irapuato, GTO, México

[b]Food Technology Department. Universitat Politècnica de València. C/ Camí de Vera s/n, 46022 València, Spain

[c]Institut de Recerca i Tecnologia Agroalimentàries (IRTA). Food Technology Center. Finca Camps i Armet, 17121 Monells, Girona, Spain

[*]Corresponding author. Tel.: +34 96 387 91 48; Fax: +34 96 387 98 39

E-mail address: gclemen@tal.upv.es (G. Clemente)

Abstract

Four models were used to simulate nitrite uptake and water loss during pork meat curing with sodium nitrite: three empirical ones (the Azuara, the Peleg and the Zugarramurdi and Lupin) and one theoretical (the diffusional).

By means of the Azuara and the Peleg models, the equilibrium moisture content and the equilibrium nitrite content were properly identified.

Zugarramurdi and Lupin's model did not provide information about process parameters.

The effective diffusivities of water (D_{we}) and nitrite (D_{Ne}) were calculated. The activation energy (E_{Na} and E_{wa}) was evaluated from the parameters of both the Peleg and the diffusional models. The results were similar; the Peleg model having the advantage of simplicity of calculation.

The effect of meat anisotropy was confirmed from the diffusional model; the perpendicular transport of nitrite is easier than the parallel.

This study highlighted the importance of choosing the most appropriate model depending on the objective to be achieved.

Keywords

Modelling, nitrite, water, diffusion, pork meat

1. Introduction

Nitrate and nitrite are present in the human diet in two ways: as nutrients in many vegetables and as food preservation substances (Sindelar and Milkowski 2012). Nitrites are added to meat products for different reasons, such as for the purposes of inhibiting potentially pathogenic microorganisms, stabilizing the product's color during curing, acting as an antioxidant or developing the typical aroma and flavor of these products (Honikel, 2008; Hospital et al., 2012). In the last few years, however, there has been growing controversy surrounding nitrate and nitrite safety in the human diet (Sindelar and Milkowski 2012). On the one hand, different studies highlight the contribution of nitrites to human nutrition and their therapeutic potential to prevent cerebrovascular accidents, myocardial infarction, hypertension or gastric ulceration (Lundberg and Weitzberg, 2009; Lundberg et al., 2008; Rocha et al., 2011). Bedale et al. (2016) point out that dietary nitrate and nitrite have positive health attributes associated with nitric oxide metabolism that are only now being understood. On the other hand, some epidemiological studies associate the ingestion of red and processed meats with colorectal cancer (Abid et al., 2014). The association with processed meats is partially attributed to nitrosamines, which are formed by the action of nitrites through a reaction with secondary amines in an acidic environment, such as that present in the stomach (Butler, 2015). However, according to Butler (2015), the presence of nitrites in food does not represent a health hazard. This author could find no substantial epidemiological evidence of a correlation between nitrosamine formation and the incidence of gastric cancers.

In the EU, potassium and sodium nitrite are currently restricted by Regulation no. 1129/2011 (Commission Regulation (EC) No 1129/2011), which is urging the meat industry to modify the technologies used in cured meat production in order to reduce the nitrites added to meat products. Nevertheless, this reduction could affect the quality and safety of cured products (Dineen et al., 2000). It is, thus, essential to monitor the curing process, which implies a better understanding of nitrite uptake kinetics and the factors governing the process (e.g. temperature).

To this end, mathematical models are very useful due to the cost and time involved in experimental salting and curing studies (Chabbouh et al., 2012).

Models in general, and those for salting and curing processes in particular, can be classified as theoretical or empirical. Theoretical models are developed from mass and energy balances, considering the principles of chemistry, physics and biology (Gómez et al., 2015a). Of these models, the diffusional ones are widely used for meat salting and curing. Usually, water diffusion and salt diffusion are considered separately and an effective diffusivity is calculated for both substances (Uribe et al., 2011; Chabbouh et al., 2012; Gómez et al., 2015b; Gómez et al., 2017).

Empirical models are not based on general or specific laws. As a general rule, the simpler the model, the easier its mathematical solution (Gómez et al., 2015a). In fact, the main advantage of empirical models is that no complex mathematical algorithms are needed, shortening the calculation time with a reasonably good description of the process. Of the empirical models used to describe meat salting and curing, Azuara's model (Schmidt et al., 2009; Corzo et al., 2012), Peleg's model (Corzo et al., 2012; Chabbouh et al., 2012) and Zugarramurdi and Lupin's model (Chabbouh et al., 2012; Corzo et al., 2013) are worth highlighting.

As Gómez et al. (2015a) points out, the level of complexity needed in a model depends on the objective to be reached. A compromise between the simplicity of the model and a good description of the experimental results should be guaranteed; thus, it is advisable to analyze the model to be used in each case according to the objective of the study to be carried out.

Based on what has been mentioned above, the objective of this study is to test different models with which to simulate nitrite gain and water loss kinetics during the curing of pork meat in a saturated brine of sodium nitrite at different temperatures prior to the optimization of the operating conditions.

2. Materials and methods

2.1 Raw material

Eight pork legs from different animals were selected from a local slaughterhouse (average weight, 9.6±1.2 kg; pH 45 minutes *post mortem* > 6.0 and pH 24 hours *post mortem* = 5.9 ± 0.1, measured in *Semimembranosus*, SM, muscle). The legs were wrapped in a polyvinyl chloride film and stored at 2 ± 1ºC for 13-14 h before separating the SM muscle from each leg. Twelve cylinders, 8.4 cm in height and 2.4 cm in diameter, were obtained from each muscle, keeping the orientation of the meat fibers parallel to the cylinder axis, as explained in Gómez et al. (2017).

2.2 Curing of the meat pork

The curing of meat cylinders was carried out in duplicate at four temperatures (0, 4, 8 and 12 ºC), as in experiment II by Gómez et al. (2017), although $NaNO_2$ was used as a curing agent instead of $NaNO_3$.

For each temperature and replication, ten of the twelve cylinders obtained from a muscle were used for curing with a saturated brine of sodium nitrite ($NaNO_2$). Another cylinder was used to determine the equilibrium concentration of nitrite and water (7 days of immersion) and the remaining one was used to characterize the initial conditions of the meat. A total of 96 cylinders were analyzed: 8 for initial conditions, 8 for equilibrium concentration and 80 for the experimental kinetics. The brine was prepared with an excess of $NaNO_2$ in order to compensate for the amount of salt absorbed by the meat.

The curing process lasted 5 days; one cylinder was removed from the brine every 12 hours and, by using a bore, two sections were obtained: an internal (1.2 cm diameter) and an external one. The evolution of the nitrite and water content of both sections over time was determined.

2.3 Analytical techniques

2.3.1. pH determination

The pH at 45 minutes *post mortem* and 24 hours *post mortem* was recorded in the slaughterhouse directly in six points of the muscle using a lab pH-meter for solids (Mattäus pH-STAR CPU, Pötmes, Germany) with a glass electrode protected by a stainless steel jacket. The pH meter was calibrated in buffers of pH 4.6 and 7.0. The device automatically corrected pH values, taking into account muscle temperature.

2.3.2. Water content.

Both the initial water content and the evolution of the water content of each cylinder section over time were determined by the AOAC methodology (AOAC, 1997). The determinations were carried out in duplicate.

2.3.3. Nitrite determination

The nitrite concentration was determined following the procedure described in Gómez et al. (2015b).

2.4. Modelling

Four models were used to model the experimental curing kinetics. The goodness of fit was evaluated for all of them by means of the percentage of explained variance (%var) and the mean relative error (%EMR).

2.4.1. Azuara´s model

Azuara et al. (1992) proposed a model for both water loss (equation 1) and salt uptake (equation 2).

$$\frac{t}{w} = \frac{1}{k_{Aw} w_e} + \frac{t}{w_e} \tag{1}$$

$$\frac{t}{s} = \frac{1}{k_{As} s_e} + \frac{t}{s_e} \tag{2}$$

2.4.2. Peleg´s model

Peleg's model (Peleg, 1988) is widely used in food processing. Equations 3 and 4 show the water loss and the salt uptake during curing, respectively.

$$\frac{t}{X - X_0} = k_1 - k_2 t \tag{3}$$

$$\frac{t}{X_s - X_{s0}} = k_3 + k_4 t \quad (4)$$

The equilibrium moisture content can be calculated from Peleg's constant, k_2 (Equation 5). In the same way, the equilibrium salt content can be calculated from k_4 (Equation 6).

$$X_e = X_0 - \frac{1}{k_2} \quad (5)$$

$$X_{se} = X_{s0} + \frac{1}{k_4} \quad (6)$$

2.4.3. Zugarramurdi and Lupin's model

Zugarramurdi and Lupin (1980) proposed a model for the curing process. Equation 7 describes water loss and salt uptake is described by Equation 8.

$$X = X_0 \exp(-k_{Zw} t) + X_e (1 - \exp(-k_{Zw} t)) \quad (7)$$

$$X_s = X_{s0} \exp(-k_{Zs} t) + X_{se} (1 - \exp(-k_{Zs} t)) \quad (8)$$

2.4.4. Diffusional model

A simplified diffusional model based on Fick´s second law was used to describe the experimental curing kinetics. The following assumptions were made:

- at the beginning of the curing process, the concentrations of water and nitrite are constant and homogeneous in the meat samples
- one-dimensional transport perpendicular to the meat fibers takes place, implying an infinite cylinder geometry.
- the external resistance to mass transfer is negligible
- the solid is homogeneous and isotropic
- the effective diffusivity is constant
- the dimensions of the samples are constant throughout the experiment

The solution of the governing equation that considers both the initial and boundary conditions described above gives Equations 9 and 10.

$$\frac{C(r,t)-C_e}{C_0-C_e}=2\sum_{n=1}^{\infty}\frac{e^{-D_e\lambda_n^2 t}}{\lambda_n R J_1(\lambda_n R)}J_0(\lambda_n r) \tag{9}$$

$$\lambda_n/J_0(\lambda_n R)=0 \tag{10}$$

where λ_n represents the characteristic values (m^{-1}).

The average nitrite and water content for both the internal cylinder (I) and the external section (E) at a given time was calculated by integrating Equation 9 between 0 and R/2 for section I, and between R/2 and R for section E. A detailed description of the calculation can be found in Gómez et al. (2017).

To estimate the effective diffusivity, an optimization problem was formulated. The SOLVER tool of EXCEL™ (Microsoft Excel) was applied to solve this optimization problem, which uses a non-linear optimization method, namely the generalized reduced gradient. The nitrite diffusivity (D_{Ne}) and water diffusivity of (D_{We}) were calculated by minimizing the mean of the squared differences between the experimental and calculated concentrations, using the model.

2.4.5. Influence of temperature on model parameters

The influence of temperature on the water and nitrite transport was determined by applying the Arrhenius equation.

3. Results and discussion

3.1 Water content

The experimental average moisture content of the two cylinder sections during the curing process at different temperatures is shown in Fig. 1. It can be observed that the moisture content in both cylinder sections dropped when the curing time lengthened and the temperature rose. The moisture content fell more quickly during the first 2 days, thereafter remaining nearly constant. As expected, during this initial period, the external section, in contact with the brine, presented a faster dehydration than the internal one; thus, the first part of the curve shows a more marked slope. In this same period, the temperature was observed to exert an influence in both cylindrical sections, so that the higher the curing temperature, the greater the initial moisture loss. The same behavior has been observed in previous research studies on curing (Gómez et al., 2015b; Gómez et al., 2017). The equilibrium moisture content of the meat samples after 3 days of curing was 0.84 kg water/kg dry matter for 0ºC and 4ºC in both sections, while for 8ºC and 12ºC, it was 0.75 kg water/kg dry matter. Similar values were obtained by Gómez et al. (2015b) when curing pork meat with sodium nitrite ($NaNO_2$) perpendicularly to meat fiber.

3.2 Nitrite content

The experimental results for the nitrite content of the two cylinder sections are shown in Fig. 2. A faster increase in the nitrite content of the external cylinder was observed at every experimental temperature during the first day of curing, whereas this increase was slower in the internal cylinder. There are two factors behind this rapid movement of the nitrite on the meat cylinder surface in the initial period: first, the large concentration gradient between the meat surface and the brine at the beginning of the curing process and, second, the high moisture content of the samples (Fig. 1), which easily facilitates nitrite diffusion in meat (Gómez et al., 2015b). Other authors reported that salt intake and water loss occurred simultaneously during curing and these two events mutually affected each other (Akköse and Aktas, 2014). Temperature was observed to have an effect on nitrite transport, increasing the nitrite content of the samples as the temperature rose. At the end of the studied period, the nitrite concentrations in the internal and external sections were similar, with values close to equilibrium: 160.5 g nitrite/L (0.13 kg nitrite/kg dry matter) at 0ºC, 173.3 g nitrite/L (0.15 kg nitrite/kg dry matter) at 4ºC, 181.6 g nitrite/L (0.14 kg nitrite/kg dry matter) at 8ºC and 197.55 g nitrite/L (0.15 kg nitrite/kg dry matter) at 12ºC, indicating that a homogeneous distribution of the sodium nitrite was attained.

3.3. Mathematical modelling

The experimental results were modelled from the average experimental kinetics data. Tables 1, 2 and 3 show the results for the empirical models. A good fit was obtained between the experimental and calculated data, as confirmed by the percentage of explained variance, which was higher than 94% for every experiment, and the mean relative error, which was lower than 10%. In Figure 3, the fit between experimental and calculated values for the three empirical models is presented. As can be observed, all the values are close to the diagonal (R^2 = 0.86 for water content and R^2 = 0.93 for nitrite content) which confirms the good agreement between the experimental kinetics and the values calculated by means of the empirical models.

The equilibrium moisture content (X_e) and the equilibrium nitrite content (X_{se}) obtained from Azuara's model coincide with the experimental values. The equilibrium values obtained by means of Peleg's model ranged between 0.68 and 0.69 kg water/kg dry matter and 0.15 and 0.16 kg nitrite/kg dry matter, respectively, which also agree with the experimental ones. It can be thus stated that both models are useful for determining the equilibrium values under the experimental conditions of this study.

The values obtained for the models' parameters are of the same order as the ones found in the literature concerning meat products (Chabbou et al., 2012; Corzo et al., 2012; Corzo et al., 2013).

A key aspect when modeling is to determine the influence of the process parameters on the results. In this study, the experimental kinetics were determined at four temperatures; thus, the influence of temperature on the parameters of the model has to be achieved. For both the Azuara and the Zugarramurdi and Lupin models, no relationship was found between either models' parameters and the temperature (Tables 1 and 3). However, in the case of the k_1 and k_3 parameters from Peleg's model, the higher the temperature, the lower they were. Specifically, the influence of temperature was assessed by means of an Arrhenius equation. Furthermore, the activation energy for water (E_{wa}) and nitrite (E_{Na}) were 51.11 kJ/mol (R^2= 0.93, EMR = 8.09 %) and 20.17 kJ/mol (R^2 = 0.99, EMR = 1,20 %), respectively. These results agree with others found in the literature (Gómez et al 2017; Gómez et al., 2015b; Gou et al., 2003).

The results from the diffusional model are shown in Table 4, while Figure 4 shows the fit between the experimental values and the ones calculated using this model. As can be observed in Figure 4, a good fit is obtained between the experimental and calculated values (R^2 = 0.95 for water content and R^2 = 0.95 for nitrite content); moreover, the percentage of explained variance is high and the percentage of mean relative errors is low (Table 4), all of which allows us to state that the proposed diffusional model is good for describing meat curing kinetics.

Both water and nitrite diffusion coefficients in Table 4 increased when the temperature rose. This effect has been observed by other authors during salting and curing experiments for the diffusion of salts (Gómez et al 2017; Gómez et al., 2015b; Telis et al., 2003; Pinotti et al., 2002) and water (Gómez et al 2017; Gómez et al., 2015b; Gou et al., 2003). The activation energy results obtained by means of the Arrhenius equation were 54.17 kJ/mol for water (E_{wa}, R^2 = 0.96, EMR = 7.10 %) and 17.57 kJ/mol for nitrite (E_{Na}, R^2 =0.98, EMR = 1.32 %). These results are similar to the ones obtained by using Peleg's model and are also in agreement with others found in the literature on pork meat (Gómez et al 2017; Gómez et al., 2015b; Gou et al., 2003). Peleg's model has the advantage of allowing the activation energy to be calculated in a simpler way. This has been pointed out by other authors while studying the drying process (Clemente et al., 2014).

Tables 5 and 6 gather the effective diffusivity values obtained by other authors working on meat products. As can be observed, they are of the same order of magnitude as the ones obtained in this study.

It must be pointed out that the diffusion of water and nitrite depends on their direction with respect to the meat fiber. When the results obtained in the present study by means of the diffusional model are compared with the ones obtained by Gómez et al. (2015b) for nitrite and water diffusion during curing parallel to the meat fibers, we can observe that the effective diffusivity for water is greater in this direction than when it takes place perpendicularly to them; in the case of nitrite, the opposite is true. This behavior was also observed for nitrate curing (Gómez et al., 2017). Gómez et al (2017) suggest that when curing parallel to the meat fibers, greater dehydration is produced, limiting the salt movement. For that reason, nitrite transport is slower when cured parallel to the meat fibers than when it takes place perpendicularly.

If the results of nitrite diffusion coefficients are compared with the ones found by Gómez et al. (2017) for nitrates obtained perpendicularly by using the same model, the nitrite values are higher than the nitrate. Considering that nitrite has a lower molecular weight than nitrate, a higher diffusion coefficient is expected for the former.

As to the activation energy, the values for parallel diffusion (Gómez et al., 2015b) were 60.32 kJ/mol for nitrite and 32.24 kJ/mol for water; thus, nitrite needs more energy for parallel diffusion than for perpendicular. When curing perpendicularly to the meat fibers, the slower movement of water produces less dehydration, facilitating the diffusion of nitrites and, consequently, the effective diffusion is greater than when it takes place parallelly. The same behavior was observed by Gómez et al. (2017) studying nitrate diffusion. These results underline the importance of the anisotropy of meat when modelling curing processes, and the effect of water movement on nitrite diffusion. Nevertheless, further studies are needed to evaluate the effect of dry curing compared to brine curing.

Gómez et al. (2017) found activation energy values of 31.86 kJ/mol for nitrate and 24.71 kJ/mol for water during nitrate diffusion perpendicular to meat fibers. As pointed out above, due to its lower molecular weight, the diffusion coefficients for nitrite are higher than for nitrate. As a consequence, if the diffusion is faster, less activation energy is needed for nitrite than for nitrate. Thus, the salt used during the curing process has an influence on it.

4. Conclusions

A good agreement was found between the experimental curing kinetics and the values calculated by means of the four models considered. Nevertheless, each model offered different information.

All the models provide information about the influence of the process parameters on the curing process, except the Zugarramurdi and Lupin model. From both Azuara's and Peleg's models, the predicted equilibrium moisture content and equilibrium nitrite content coincided with the experimental values.

According to the diffusional model, the perpendicular nitrite diffusion coefficient was higher than that of nitrate calculated in a previous study.

The activation energy for water and nitrite determined from the parameters of both the Peleg and the diffusional models was similar. However, the Peleg model had the advantage of simplicity of calculation. The values of the activation energy and the effective diffusivity confirm the effect of meat anisotropy during curing; the perpendicular transport of nitrite is easier than the parallel.

The above conclusions highlight that when modeling the curing process, it is important to choose the most appropriate model depending on the objective of the study.

NOMENCLATURE

C	Moisture or nitrite concentration	$kg*m^{-3}$
C_0	Initial concentration of nitrite or water	$kg*m^{-3}$
C_e	Equilibrium concentration of nitrite or water	$kg*m^{-3}$
D_e	Effective diffusivity	m^2*s^{-1}
k_{As}	Azuara's model parameter	day^{-1}
k_{Aw}	Azuara's model parameter	day^{-1}
k_{Zw}	Zugarramurdi and Lupin's model parameter	day^{-1}

k_{Zs}	Zugarramurdi and Lupin's model parameter	day^{-1}
k_1	Peleg's model parameter	day*g dry matter*g $water^{-1}$
k_2	Peleg's model parameter	g dry matter*g $water^{-1}$
k_3	Peleg's model parameter	day*g dry matter* g $nitrite^{-1}$
k_4	Peleg's model parameter	g dry matter*g $nitrite^{-1}$
R	Radius of the cylinder	m
r	Radial coordinate	m
s	Nitrite content	g nitrite*(g initial $sample)^{-1}$
s_e	Equilibrium nitrite content	g nitrite*(g initial $sample)^{-1}$
t	Time (diffusional model)	s
t	Time (empirical models)	day
w	Moisture content	g water*(g initial $sample)^{-1}$
w_e	Equilibrium moisture content	g water*(g initial $sample)^{-1}$
X	Moisture content	kg water*(kg dry $matter)^{-1}$
X_e	Equilibrium moisture content	kg water*(kg dry $matter)^{-1}$
X_0	Initial moisture content	kg water*(kg dry $matter)^{-1}$
X_s	Nitrite content	kg nitrite*(kg dry $matter)^{-1}$
X_{se}	Equilibrium nitrite content	kg nitrite*(kg dry $matter)^{-1}$
X_{s0}	Initial nitrite content	kg nitrite*(kg dry $matter)^{-1}$

ACKNOWLEDGEMENTS

The authors of this paper acknowledge the financial support from CONSOLIDER INGENIO 2010 (CSD2007-00016), Spain.

REFERENCES

Abid, Z., Cross, A. J., & Sinha, R. (2014). Meat, dairy, and cancer. *American Journal of Clinical Nutrition*, 100(1), 386S–393S.

Akköse, A. & Aktaş, N. (2014). Curing and diffusion coefficient study in pastırma, a Turkish traditional meat product. *Meat Science,* 96 (1), 311–314.

AOAC. (1997). Official methods of analysis of the Association of Official Analytical Chemists International (16th ed., 3rd revision). Gaithersburg, USA.

Azuara, E., Cortes, R., Garcia, H. S. & Beristain, C. I. (1992). Kinetic-model for osmotic dehydration and its relationship with Fick 2nd law, *International Journal of Food Science and Technology,* 27(4), 409-418.

Bedale, W., Sindelar, J.J. & Milkowski, A.L. (2016). Dietary nitrate and nitrite: Benefits, risks, and evolving perceptions. *Meat Science*, 120, 85-92.

Boudhrioua, N., Djendoubi, N., Bellagha, S. & Kechaou, N. (2009). Study of moisture and salt transfers during salting of sardine fillets. *Journal of Food Engineering*, 94(1), 83-89.

Butler, A. (2015). Nitrites and nitrates in the human diet: Carcinogens or beneficial hypotensive agents? *Journal of Ethnopharmacology*, 167(5), 105-107

Chabbouh, M., Ahmed, S.B.H., Farhat, A., Sahli, A. & Bellagha, S. (2012). Studies on the salting step of Tunisian kaddid meat: Experimental kinetics, modeling and quality. *Food and Bioprocess Technology*, 5(5), 1882-1895.

Clemente, G., Sanjuán, N., Cárcel, J.A. & Mulet, A. (2014). Influence of temperature, air velocity and ultrasound application on drying kinetics of grape seeds. *Drying Technology*, 32(1), 68-76.

Commission Regulation (EC) No 1129/2011. (2011). Commission Regulation (EC) No1129/2011 of 11 November 2011 amending Annex II to Regulation (EC) No 1333/2008 of the European Parliament and of the Council by establishing a Union list of Food Additives.

Corzo, O., Bracho, N. & Rodríguez, J. (2012). Comparison of Peleg and Azuara et al. models in the modeling mass transfer during pile salting of goat sheets, *LWT-Food Science and Technology*, 46(2), 448-452.

Corzo, O., Bracho, N. & Rodríguez, J. (2013). Pile salting kinetics of goat sheets using Zugarramurdi and Lupin's model. *Journal of Food Processing and Preservation*, 37, 615-620.

Dineen N.M., Kerry J.P., Lynch P.B., Buckley D.J., Morrissey P.A. & Arendt E.K. (2000). Reduced nitrite levels and dietary α-tocopheryl acetate supplementation: effects on the colour and oxidative stability of cooked hams. *Meat Science*, 55(4), 475-482.

Gómez, J., Clemente, G. & Sanjuán, N. (2015a). Review of mathematical models to describe the food salting process. *DYNA* 82(190), 23-30.

Gómez, J., Sanjuán, N., Bon, J., Arnau, J. & Clemente, G. (2015b). Effect of temperature on nitrite and water diffusion in pork meat. *Journal of Food Engineering*, 149, 188-194.

Gómez, J., Sanjuán, N., Arnau, J., Bon, J. & Clemente, G. (2017). Diffusion of nitrate and water in pork meat: Effect of the direction of the meat fiber. Journal of Food Engineering, 214, 69-78.

Gou, P., Comaposada, J. & Arnau, J. (2003). NaCl content and temperatura effects on moisture diffusivity in the Gluteus medius muscle of pork ham. *Meat Science*, 63(1), 29-34.

Honikel, K. O. (2008). The use and control of nitrate and nitrite for the processing of meat products. *Meat Science*, 78(1-2), 68-76.

Hospital, X.F., Hierro, E. & Fernández M. (2012). Survival of Listeria innocua in dry fermented sausages and changes in the typical microbiota and volatile profile as affected by the concentration of nitrate and nitrite. *International Journal of Food Microbiology*, 153(3), 395-401.

Lundberg, J. O., Weitzberg, E. & Gladwin, M. T. (2008). The nitrate-nitrite-nitric oxide pathway in physiology and therapeutics. *Nature Reviews Drug Discovery*, 7(2), 156-167.

Lundberg, J. O. & Weitzberg, E. (2009). NO Generation from inorganic nitrate and nitrite: Role in physiology, nutrition and therapeutics. *Archives of Pharmacal Research,* 32(8), 1119-1126.

Peleg, M. (1988). An empirical-model for the description of moisture sorption curves. *Journal of Food Science*, 53(4), 1216.

Pinotti, A., Graiver, N., Califano A., & Zaritzky, N. (2002). Diffusion of nitrite and nitrate salts in pork tissue in the presence of sodium chloride. *Journal of Food Science*, 67(6), 2165-2171

Rocha, B. S., Gago, B., Pereira, C., Barbosa, R. M., Bartesaghi, S., Lundberg, J. O., et al. (2011). Dietary nitrite in nitric oxide biology: A redox interplay with implications for pathophysiology and therapeutics. *Current Drug Targets*, 12(9), 1351-1363.

Schmidt, F.C., Carciofi, B.A.M. & Laurindo, J.B. (2009). Application of diffusive and empirical models to hydration, dehydration and salt gain during osmotic treatment of chicken breast cuts. *Journal of Food Engineering*, 91, 553-559.

Sindelar, J.J. & Milkowski, A.L. (2012). Human safety controversies surrounding nitrate and nitrite in the diet. *Nitric Oxide*, 26, 259-266.

Siró, I., Vén, Cs., Balla, Cs., Jónás, G., Zeke, I. & Friedrich, L. (2009). Application of an ultrasonic assisted curing technique for improving the diffusion of sodium chloride in porcine meat. *Journal of Food Engineering*, 91, 353-362.

Telis, V.R.N., Romanelli, P.F., Gabas, A.L. & Telis-Romero, J. (2003). Salting kinetics and salt diffusivities in farmed pantanal caiman muscle. *Pesquisa Agropecuaria Brasileira* 38(4), 529–535.

Uribe, E., Miranda, M., Vega-Galvez, A., Quispe, I., Claveria, R. & Di Scala, K. (2011). Mass transfer modelling during osmotic dehydration of jumbo squid (*Dosidicus gigas*): Influence of temperature on diffusion coefficients and kinetic parameters. *Food and Bioprocess Technology, 4*(2), 320-326.

Volpato, G., Michielin, E.M.Z., Ferreira, S.R.S. & Petrus, J.C.C. (2007). Kinetics of the diffusion of sodium chloride in chicken breast (Pectoralis major) during curing. *Journal of Food Engineering,* 79(3), 779–785.

Zugarramurdi, A. & Lupin, H.M. (1980). A model to explain observed behaviour on fish salting. *Journal of Food Science*, 45, 1305–1311.

FIGURE CAPTIONS

Fig. 1. Kinetics of water loss in cylindrical samples during salting at different temperatures perpendicular to meat fibers. a) Internal cylinder, b) External cylinder.

Fig. 2. Kinetics of nitrite gain in cylindrical samples during salting at different temperatures perpendicular to meat fibers. a) Internal cylinder, b) External cylinder.

Fig. 3. Fit between experimental and calculated values for empirical models. a) Water content (kg water/kg dm), b) Nitrite content (g nitrite/L).

Fig. 4. Fit between experimental and calculated values for diffusional model. a) Water content (kg water/kg dm), b) Nitrite content (g nitrite/L).

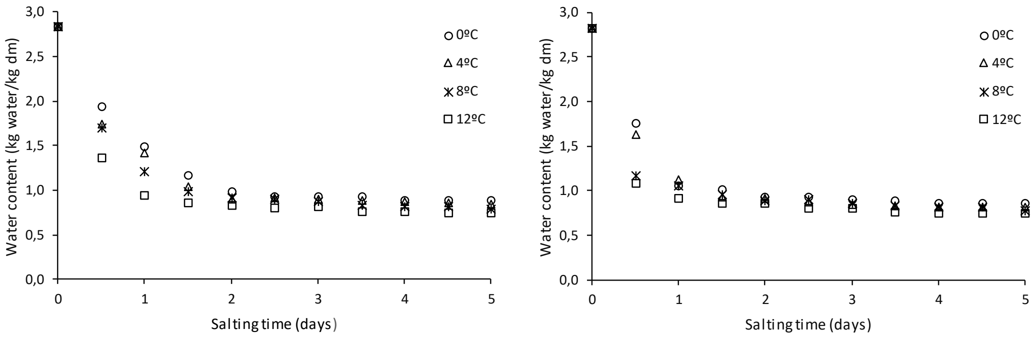

Water content (kg water/kg dm)
Salting time (days)
0ºC
4ºC
8ºC
12ºC
3,0
2,5
2,0
1,5
1,0
0,5
0,0
0
1
2
3
4
5

(a) (b)

Fig. 1.

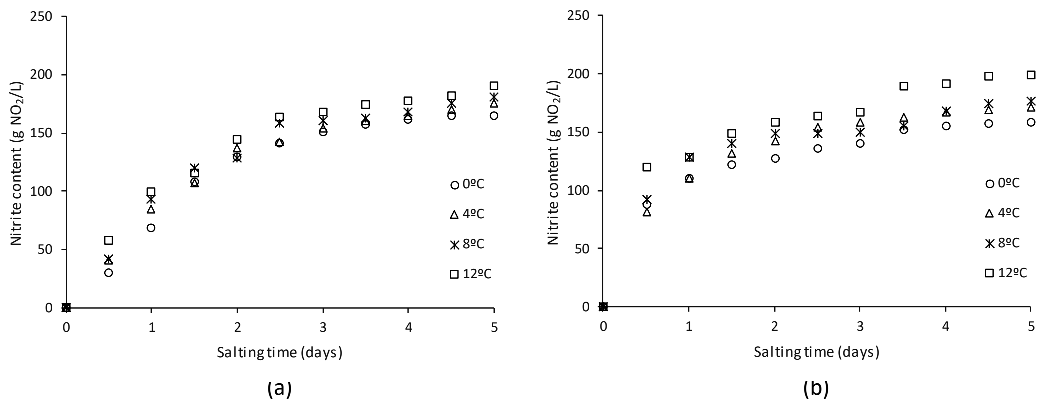
250
200
150
100
50
0
Nitrite content (g NO2/L)
0ºC
4ºC
8ºC
12ºC
0
1
2
3
4
5
Salting time (days)
(a)
250
200
150
100
50
0
Nitrite content (g NO2/L)
0ºC
4ºC
8ºC
12ºC
0
1
2
3
4
5
Salting time (days)
(b)

Fig. 2.

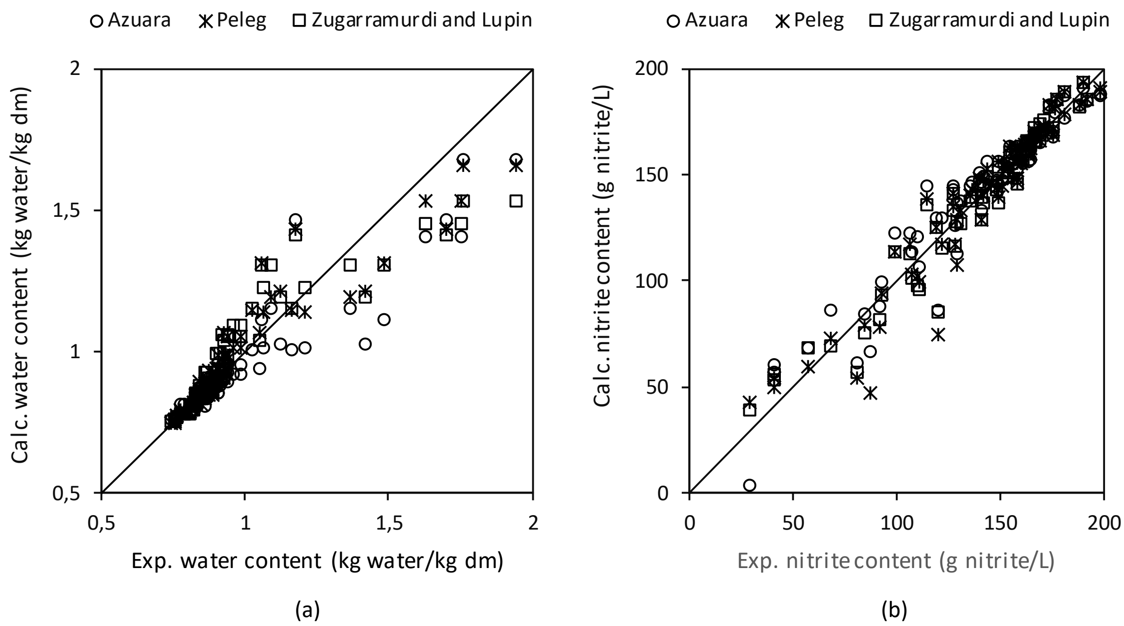
Azuara
Peleg
Zugarramurdi and Lupin
Calc. water content (kg water/kg dm)
Exp. water content (kg water/kg dm)
0,5
1
1,5
2
(a)
Azuara
Peleg
Zugarramurdi and Lupin
Calc. nitrite content (g nitrite/L)
Exp. nitrite content (g nitrite/L)
0
50
100
150
200
(b)

Fig. 3.

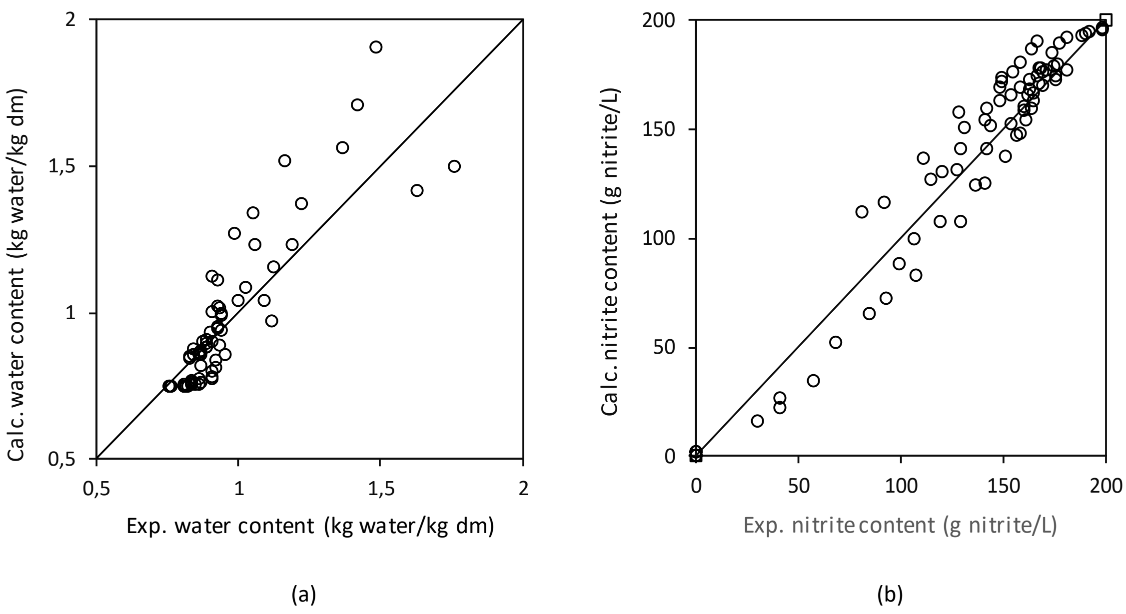

2
1,5
1
0,5
0,5
1
1,5
2
Calc. water content (kg water/kg dm)
Exp. water content (kg water/kg dm)
(a)
200
150
100
50
0
0
50
100
150
200
Calc. nitrite content (g nitrite/L)
Exp. nitrite content (g nitrite/L)
(b)

Fig. 4.

TABLE CAPTIONS

Table 1. Parameters of Azuara's model

Table 2. Parameters of Peleg's model

Table 3. Parameters of Zugarramurdi and Lupin's model

Table 4. Parameters of the diffusional model

Table 5. Literature values of diffusion coefficients (m^2/s) for different salts during the curing process.

Table 6. Literature values of diffusion coefficients (m^2/s) for water during the salting process.

Table 1.

T ºC	k_{Aw} day^{-1}	X_e kg w*kg dm^{-1}	%var	%EMR	k_{As} day^{-1}	X_{se} kg n/kg dm^{-1}	%var	%EMR
0	4.43	0.84	96.22	4.18	3.66	0.15	94.81	10.04
4	4.70	0.81	94.74	5.44	4.01	0.15	97.49	6.04
8	4.26	0.78	96.90	5.19	4.86	0.15	97.11	6.52
12	5.49	0.73	99.04	3.46	3.30	0.15	94.13	7.40

Table 2.

T ºC	k_1 day*g dm*g w^{-1}	k_2 g dm*g w^{-1}	%var	%EMR	k_3 day*g dm* g n^{-1}	k_4 g dm*g n^{-1}	%var	%EMR
0	0.19	0.46	96.47	6.09	2.71	6.51	94.97	7.89
4	0.15	0.47	97.77	5.36	2.45	6.47	97.40	5.72
8	0.13	0.47	97.55	3.86	2.09	6.68	96.91	6.24
12	0.07	0.47	99.28	2.51	1.89	6.36	93.73	6.72

Table 3.

T ºC	k_{zw} day^{-1}	%var	%EMR	k_{zs} day^{-1}	%var	%EMR
0	0.79	94.85	6.44	1.23	99.70	6.34
4	1.11	97.18	4.84	0.57	99.58	6.13
8	0.66	96.84	5.61	1.14	99.53	7.70
12	1.16	98.62	4.10	0.58	99.21	7.41

Table 4.

T ºC	D_{we} *10^{10} m^2s^{-1}	%var	%EMR	D_{Ne} *10^{10} m^2s^{-1}	%var	%EMR
0	1.95	90.02	9.74	1.38	92.96	8.93
4	2.45	91.02	8.08	1.61	93.59	9.16
8	3.30	95.84	9.43	1.74	93.64	8.74
12	5.40	98.73	5.20	1.93	93.21	8.70

Table 5.

PRODUCT	SALT	$D*10^{10}$	REFERENCE
Pork	$NaNO_3$	0.007-1.41	Gómez et al. (2017)
Pork	$NaNO_2$	0.04-0.11	Gómez et al. (2015b)
Pork	NaCl	2.40	Siró et al. (2009)
Chicken	NaCl	8.99-9.55	Volpato et al. (2007)
Pork	$NaNO_2$,KNO_3	3.80-9.50	Pinotti et al (2002)

Table 6.

PRODUCT	SALT	$D*10^{10}$	REFERENCE
Pork	$NaNO_3$	52.20-124.60	Gómez et al. (2017)
Pork	$NaNO_2$	59.40-97.33	Gómez et al. (2015b)
Sardine	NaCl	2.43-109.00	Boudhrioua et al. (2009)